

Divergence Regulated Encoder Network for Joint Dimensionality Reduction and Classification

Joshua Peeples^{*} Sarah Walker Connor McCurley Alina Zare
 Department of Electrical & Computer Engineering
 University of Florida, Gainesville, FL, 32611, USA
 {jpeeples, sarah.walker, cmccurley, azare}@ufl.edu

James Keller
 Department of Electrical Engineering & Computer Science
 University of Missouri, Columbia, MO, 65211, USA
 KellerJ@missouri.edu

Abstract

In this paper, we investigate performing joint dimensionality reduction and classification using a novel histogram neural network. Motivated by a popular dimensionality reduction approach, t-Distributed Stochastic Neighbor Embedding [15] (t-SNE), our proposed method incorporates a classification loss computed on samples in a low-dimensional embedding space. We compare the learned sample embeddings against coordinates found by t-SNE in terms of classification accuracy and qualitative assessment. We also explore use of various divergence measures in the t-SNE objective. The proposed method has several advantages such as readily embedding out-of-sample points and reducing feature dimensionality while retaining class discriminability. Our results show that the proposed approach maintains and/or improves classification performance and reveals characteristics of features produced by neural networks that may be helpful for other applications.

1. Introduction

Recently, deep convolutional neural network (DCNN)-based approaches have shown remarkable performance on image classification tasks [9, 21, 11]. State-of-the-art image classification networks often contain thousands or even millions of parameters which need to be learned during training. While it has been argued in the literature that high-dimensionality (data, parameterization, model complexity) is more amenable for classification [1, 4, 8, 12],

methods taking advantage of high-dimensionality are often inscrutable. One approach for handling the nuances associated with high-dimensionality is simply to reduce the dimensionality of the data/model.

Manifold Learning or Dimensionality Reduction (DR) has proven to be a critical tool in many machine learning applications, such as: visualizing data, removing redundancy, minimizing memory usage, and reducing the effects of the Curse of Dimensionality. [23, 17, 2]. The goal of manifold learning can be posed as discovering intrinsic (often lower-dimensional) features from the data which meet an overarching objective, such as: preserving variance, finding compressed representations of data, maintaining global or local structure or promoting class discriminability in the embedding space [23, 3, 26, 22]. Most studies perform classification or regression after applying unsupervised dimensionality reduction. However, it has been shown that there are advantages to learning the low-dimensional representations and classification/regression models simultaneously [5, 19]. Specific to classification, the goal of DR is to discover embedding functions that take data from the input feature space and transform it into a lower-dimensional coordinate system or *latent space*. Ideally, the low-dimensional features capture “useful” properties of the data while enforcing constraints such as topological ordering and class separability [25].

The representation of data is a critical factor in determining machine learning classification performance [3]. For images, one can generally represent information through color, shape, and texture features [10]. As shown in the literature [14], texture features often serve as the most powerful descriptor of the three. As currently constructed, DCNNs cannot directly model texture information without the

^{*}This material is based upon work supported by the National Science Foundation Graduate Research Fellowship under Grant No. DGE-1842473 and by the Office of Naval Research grant N00014-16-1-2323.

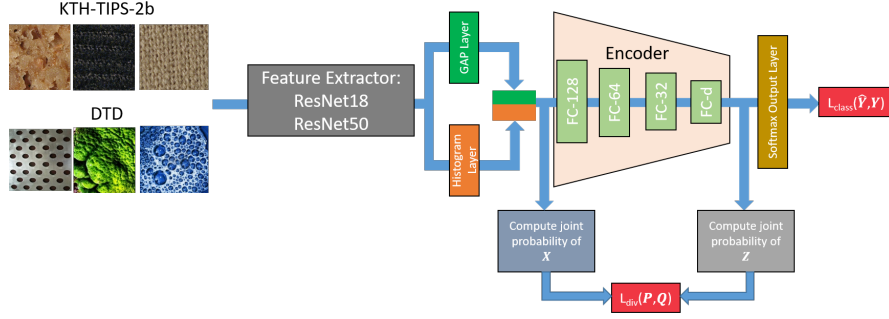


Figure 1: Architecture for the proposed divergence regulated encoder networks (DRENs).

use of extra layers and parameters. To capture texture features in DCNNs, *histogram layer* networks [18] were introduced to characterize the distribution of features in the model. We hypothesize that incorporating texture features into our proposed approach will assist in providing meaningful representations of the data for classification.

Based on these motivations, we introduce a neural classification approach which inherently learns compressed feature representations optimized for class discriminability. The contributions of this work are summarized as the following:

- We propose a neural classification scheme which finds discriminative, low-dimensional representations of the input data. The network learns from a t-SNE based objective, yet outperforms the data representations found by classical t-SNE in terms of classification accuracy.
- The proposed method is constructed from a histogram layer network backbone which extracts highly descriptive texture features.
- The proposed approach can readily embed out-of-sample points, allowing it to be applied universally to other image classification datasets. In our experiments, we verified the effectiveness of the proposed method on two datasets: KTH-TIPS-2b [16] and Describable Texture Dataset (DTD) [7].

2. Methods

2.1. Proposed Approach

In order to jointly perform classification and DR, our objective function is comprised of two terms: classification loss, L_{class} , and a divergence measure, L_{div} :

$$L_{total} = (1 - \lambda)L_{class}(\hat{\mathbf{Y}}, \mathbf{Y}) + \lambda L_{div}(\mathbf{P}, \mathbf{Q}) \quad (1)$$

where $\mathbf{P} \in \mathbb{R}^{N \times N}$ is the joint probability distribution on the high dimensional input features $\mathbf{X} \in \mathbb{R}^{N \times D}$ for N samples in a mini-batch, $\mathbf{Q} \in \mathbb{R}^{N \times N}$ is the joint probability distribution on the lower dimensional embeddings $\mathbf{Z} \in \mathbb{R}^{N \times d}$,

$\hat{\mathbf{Y}} \in \mathbb{R}^{N \times C}$ are the sample predictions for C classes, and $\mathbf{Y} \in \mathbb{R}^{N \times C}$ are the true class labels. We add a weight, λ , to leverage the contribution of each term to the overall objective. We define L_{class} as the popular cross-entropy loss:

$$L_{class}(\hat{\mathbf{Y}}, \mathbf{Y}) = -\frac{1}{N} \sum_{i=1}^N \sum_{c=1}^C y_{ic} \log \hat{y}_{ic} \quad (2)$$

For t-SNE, Kullback-Leibler (KL) divergence is typically used to minimize the divergence between the higher and lower dimensional joint probability distributions:

$$L_{div}(\mathbf{P}, \mathbf{Q}) = \sum_{i=1}^N \sum_{j=1}^N p_{ij} \log \frac{p_{ij}}{q_{ij}} \quad (3)$$

Following the standard t-SNE [15] implementation, we used a normalized radial basis kernel and Student t-distribution with a single degree of freedom to estimate the neighbor probability matrices \mathbf{P} and \mathbf{Q} in the high and low dimensional feature spaces, respectively. Our approach is agnostic to the selection of a divergence measure. Hence, we used other divergence measures such as Wassertein-1 (*i.e.*, earth mover's distance) [13] and Renyi's divergence [24] with $\alpha = 0.5$. There was not a statistically significant difference in the classification performance of our model. Therefore, results presented in this work are representative of using KL divergence.

2.2. Implementation

For our divergence regulated encoder network (DREN), we used two pretrained models as the backbones, ResNet18 and ResNet50 [9] for KTH-TIPS-2b [16] and DTD [7], respectively. We added a histogram layer after the last convolutional layer for each of the pretrained models. From these models, we extracted the high dimensional feature vectors, \mathbf{X} , for each sample. For the baseline and histogram models used for KTH-TIPS-2b and DTD, D was 512, 1024, 2048, and 4096 respectively. Our encoder was comprised of four fully connected layers of size 128, 64, 32, and d . We used

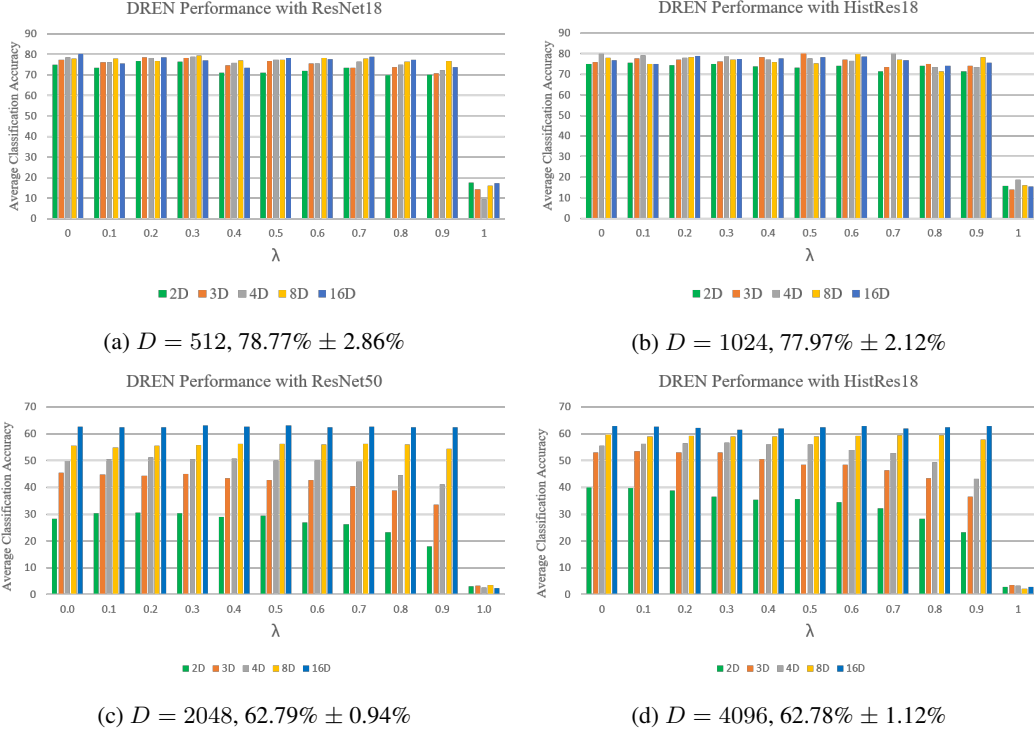


Figure 2: Encoder experiments performance of the different variations of DREN for KTH-TIPS-2b (2a-2b) and DTD (2c-2d). In each sub caption, the high dimensional size and performance without the encoder is shown. For clarity, the error bars are not shown.

ReLU activation functions for the first three layers and feed the d -dimensional embedding to a softmax output layer for classification.

The embeddings, \mathbf{Z} , were used to compute L_{div} and to update the weights of the model via backpropagation of errors. To create a fair comparison to t-SNE applied to the high dimensional features, we only updated the lower-dimensional embeddings. Therefore, \mathbf{P} was removed from the computational graph such that only the gradient information from \mathbf{Q} was used. The overall structure of DREN is shown in Figure 1 and the code for our work is publicly available [code provided in supplemental material].

3. Experimental Setup

Our experiments consisted of two main components: encoder performance and comparisons to t-SNE. For our encoder experiments, we investigated the selection of hyperparameters λ and d for the proposed DREN models. The typical train/test splits for DTD (train on 80 images per class and test on 40 images per class) and KTH-TIPS-2b (train on three samples, test on one sample) were used for our experiments [14]. We held 10% of the training data for validation and applied each model to the holdout test set. We performed four and ten runs of data splits for KTH-TIPS-2b

and DTD respectively. The average classification accuracy is reported across the different folds. We followed a similar training procedure and data augmentation from previous works [27, 18], except Adam optimization was used. We also only updated newly added layers (*i.e.*, histogram layers, encoder, output layer) and kept the pretrained weights fixed. The number of bins used in all histogram models was 16.

The weight in the objective term, λ , was varied from 0 to 1 in steps of 0.1. The embedding dimension, d , was set to 2, 3, 4, 8, and 16. After our encoder experiments, we compared the training and testing embeddings learned by DREN to t-SNE. In order to embed test samples for t-SNE, we used an approach similar to Locally Linear Embedding [20], which assumes that a sample can be represented as a linear combination of its nearest neighbors. Thus, low-dimensional coordinates of unseen test points were found as constrained combinations of their nearest neighbors in the training set. We evaluated each embedding a) qualitatively and b) quantitatively by reporting the classification accuracy of a K -NN classifier on the test data ($K = 3$).

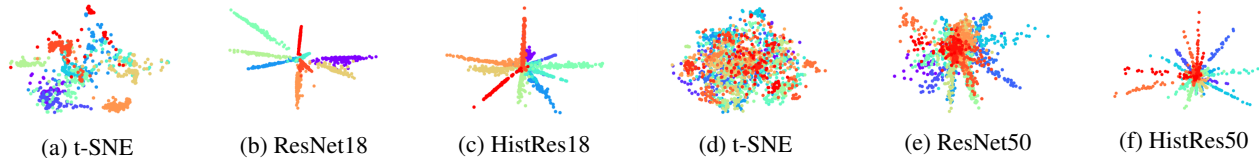


Figure 3: 2D embeddings of test images from t-SNE out-of-sample approach and different variations of DREN for KTH-TIPS-2b (3a-3c) and DTD (3d-3f). The embeddings are shown from models trained and validated on the same data. The colors represent different classes from each dataset. In the 2D space, the HistRes features are more separable according to an angular measure, and are also much more compact, *i.e.*, each class mostly varies across a single principal vector, and the principal vectors are well-separated by an angular margin.

Table 1: Test classification performance using K -NN “trained” on embeddings from t-SNE and DREN models. For the DREN models, the weight corresponding to the best average performance is reported. The best average result is bolded.

Dataset	Embedding Dimension (d)	t-SNE	DREN ResNet	DREN HistRes
KTH-TIPS-2b	2	76.70% \pm 2.88%	76.79%\pm3.18% ($\lambda = .2$)	74.60% \pm 3.47% ($\lambda = .1$)
	3	76.91% \pm 3.40%	78.18% \pm 3.40% ($\lambda = 0$)	79.23%\pm3.63% ($\lambda = .5$)
DTD	2	43.37%\pm1.01%	29.35% \pm 1.22% ($\lambda = .2$)	40.44% \pm 1.64% ($\lambda = 0$)
	3	43.55% \pm 1.22%	44.28% \pm 1.57% ($\lambda = 0$)	53.02%\pm1.24% ($\lambda = .1$)

4. Results and Discussion

4.1. Encoder Experiments

For the two hyperparameters, λ and d , the performance of the DREN models depended more on the selection of the embedding dimension. Ideally, as the dimensionality of the feature space becomes larger, inter-class separability should increase and intra-class variations should decrease leading to improved performance (as shown in our experiments for the DREN models). However, our DREN models achieved statistically comparable performance to the baseline models without an encoder at significantly lower dimensions (except for DREN with ResNet50 for DTD). Our method is also stable to the selection of λ except for when only the L_{div} is considered ($\lambda=1$). In this case, the model is an unsupervised approach and will only learn embeddings that minimize the divergence between higher and lower dimension. In our implementation, the error was not backpropagated through the output layer once $\lambda = 1$. In this instance, the output layer will not be updated, leading to poor classification performance.

In Figures 2a and 2b, the performance of the DREN models with and without the histogram layers for KTH-TIPS-2b were comparable. KTH-TIPS-2b primarily consisted of images collected in a controlled environment [14]. As a result, the local, texture features extracted by the histogram layers may not add as much information for the classification. However, the DREN models with the histogram layers performed better on DTD across the different combinations of hyperparameters as shown in Figures 2c and 2d. DTD contained images collected “in-the-wild” and also has more classes (47) than KTH-TIPS-2b (11). The em-

beddings learned by the DREN histogram models retained useful information from the texture features. nal joint probability distributions without considering class information.

4.2. t-SNE Comparisons

In Table 1, the test performance for the K -NN classifiers showed the utility of the DREN embeddings for not only visualization but also classification. Our DREN models also have an advantage over t-SNE in that new images can be embedded without a separate out-of-sample approach. In Figure 3, the t-SNE embedding of the test points are not as visually compact and separable as the DREN models. The test samples embeddings produced from the DREN models also seem to have “angular” feature distributions. As noted in other works [6], models trained using cross-entropy appear to learn these unique, intrinsic feature coordinates in comparison to the t-SNE embeddings that are learned by only using KL divergence. For the DREN histogram models, the “angular” embeddings may also be produced as a result of normalization as the features are also centered around 0. The features captured by the histogram layer binning function are naturally between 0 and 1 while the features from the global average pooling layer are followed by batch normalization [18].

5. Conclusion

In this work, we presented DREN models for joint dimensionality reduction and classification. The proposed approach learns discriminative features at lower dimensions that can be used for different tasks. The approach has several advantages and is a general framework that can use various classification/divergence measures and deep learning

models.

References

- [1] Joseph Anderson, Mikhail Belkin, Navin Goyal, Luis Rademacher, and James Voss. The more, the merrier: the blessing of dimensionality for learning large gaussian mixtures. *Journal of Machine Learning Research*, 35, 11 2013.
- [2] Etienne Becht, Leland McInnes, John Healy, Charles-Antoine Dutertre, Immanuel WH Kwok, Lai Guan Ng, Florent Ginhoux, and Evan W Newell. Dimensionality reduction for visualizing single-cell data using umap. *Nature biotechnology*, 37(1):38–44, 2019.
- [3] Y. Bengio, A. C. Courville, and P. Vincent. Unsupervised feature learning and deep learning: A review and new perspectives. *CoRR*, abs/1206.5538, 2012.
- [4] Leo Breiman. Statistical modeling: The two cultures. *Statistical Science*, 16(3):199 – 231, 2001.
- [5] G. Chao, Y. Luo, and W. Ding. Recent advances in supervised dimension reduction: A survey. *Machine Learning and Knowledge Extraction*, 1(1):341–358, 2019.
- [6] Hongjun Choi, Anirudh Som, and Pavan Turaga. Amc-loss: Angular margin contrastive loss for improved explainability in image classification. In *Proceedings of the IEEE/CVF Conference on Computer Vision and Pattern Recognition Workshops*, pages 838–839, 2020.
- [7] M. Cimpoi, S. Maji, I. Kokkinos, S. Mohamed, and A. Vedaldi. Describing textures in the wild. In *Proceedings of the IEEE Conf. on Computer Vision and Pattern Recognition (CVPR)*, 2014.
- [8] A. N. Gorban and I. Y. Tyukin. Blessing of dimensionality: mathematical foundations of the statistical physics of data. *Philosophical Transactions of the Royal Society A: Mathematical, Physical and Engineering Sciences*, 376(2118):20170237, 2018.
- [9] Kaiming He, Xiangyu Zhang, Shaoqing Ren, and Jian Sun. Deep residual learning for image recognition. *CoRR*, abs/1512.03385, 2015.
- [10] PS Hiremath and Jagadeesh Pujari. Content based image retrieval based on color, texture and shape features using image and its complement. *International Journal of Computer Science and Security*, 1(4):25–35, 2007.
- [11] G. Huang, Z. Liu, L. Van Der Maaten, and K. Q. Weinberger. Densely connected convolutional networks. In *2017 IEEE Conference on Computer Vision and Pattern Recognition (CVPR)*, pages 2261–2269, 2017.
- [12] W. Ronny Huang, Zeyad Emam, Micah Goldblum, Liam Fowl, Justin K. Terry, Furong Huang, and Tom Goldstein. Understanding generalization through visualizations. *CoRR*, abs/1906.03291, 2019.
- [13] Elizaveta Levina and Peter Bickel. The earth mover’s distance is the mallows distance: Some insights from statistics. In *Proceedings Eighth IEEE International Conference on Computer Vision. ICCV 2001*, volume 2, pages 251–256. IEEE, 2001.
- [14] Li Liu, Jie Chen, Paul Fieguth, Guoying Zhao, Rama Chellappa, and Matti Pietikäinen. From bow to cnn: Two decades of texture representation for texture classification. *International Journal of Computer Vision*, 127(1):74–109, 2019.
- [15] Laurens van der Maaten and Geoffrey Hinton. Visualizing data using t-sne. *Journal of machine learning research*, 9(Nov):2579–2605, 2008.
- [16] P Mallikarjuna, Alireza Tavakoli Targhi, Mario Fritz, Eric Hayman, Barbara Caputo, and Jan-Olof Eklundh. The kth-tips2 database. *KTH Royal Institute of Technology*, 2006.
- [17] Nikunj C. Oza and Kagan Tumer. Input decimation ensembles: Decorrelation through dimensionality reduction. In Josef Kittler and Fabio Roli, editors, *Multiple Classifier Systems*, pages 238–247, Berlin, Heidelberg, 2001. Springer Berlin Heidelberg.
- [18] Joshua Peebles, Weihuang Xu, and Alina Zare. Histogram layers for texture analysis. *arXiv preprint arXiv:2001.00215*, 2020.
- [19] I. Rish, G. Grabarnik, G. A. Cecchi, F. Pereira, and G. J. Gordon. Closed-form supervised dimensionality reduction with generalized linear models. pages 832–839, 01 2008.
- [20] S. T. Roweis and L. K. Saul. Nonlinear dimensionality reduction by locally linear embedding. *Science*, 290(5500):2323–2326, 2000.
- [21] C. Szegedy, V. Vanhoucke, S. Ioffe, J. Shlens, and Z. Wojna. Rethinking the inception architecture for computer vision. In *2016 IEEE Conference on Computer Vision and Pattern Recognition (CVPR)*, pages 2818–2826, 2016.
- [22] N. Thorstensen. *Manifold learning and applications to shape and image processing*. PhD thesis, Ecole Nationale des Ponts et Chaussees, Paris, France, Nov. 2009.
- [23] L. van der Maaten, E. Postma, and H. Herik. Dimensionality reduction: A comparative review. *Journal of Machine Learning Research - JMLR*, 10, 01 2007.
- [24] Tim Van Erven and Peter Harremoos. Rényi divergence and kullback-leibler divergence. *IEEE Transactions on Information Theory*, 60(7):3797–3820, 2014.
- [25] E. Vural and C. Guillemot. A study of the classification of low-dimensional data with supervised manifold learning. *CoRR*, abs/1507.05880, 2018.
- [26] X. Geng, D. Zhan, and Z. Zhou. Supervised nonlinear dimensionality reduction for visualization and classification. *IEEE Transactions on Systems, Man, and Cybernetics, Part B (Cybernetics)*, 35(6):1098–1107, Dec 2005.
- [27] Jia Xue, Hang Zhang, and Kristin Dana. Deep texture manifold for ground terrain recognition. In *Proceedings of the IEEE Conference on Computer Vision and Pattern Recognition*, pages 558–567, 2018.